Published in final edited form as:
Neuron. 2012 September 20; 75(6): 1022–1034. doi:10.1016/j.neuron.2012.08.002.

Excessive activation of mTOR in postnatally-generated granule cells is sufficient to cause epilepsy

Raymund Y.K. Pun[1], **Isaiah J. Rolle**[3], **Candi L. LaSarge**[1], **Bethany E. Hosford**[3], **Jules M. Rosen**[1], **Juli D. Uhl**[5], **Sarah N. Schmeltzer**[3], **Christian Faulkner**[1], **Stefanie L. Bronson**[3], **Brian L. Murphy**[3], **David A. Richards**[1,2,3], **Katherine D. Holland**[4], and **Steve C. Danzer**[1,2,3]

[1]Department of Anesthesia, Cincinnati Children's Hospital Medical Centre, Cincinnati, OH, 45229

[2]Departments of Anesthesia and Pediatrics, University of Cincinnati, Cincinnati, OH, 45267

[3]Program in Neuroscience, University of Cincinnati, Cincinnati, OH, 45267

[4]Department of Neurology, Cincinnati Children's Hospital Medical Centre, Cincinnati, OH, 45229

[5]Division of Molecular and Developmental Biology, Cincinnati Children's Hospital Medical Centre Research Foundation, Cincinnati, OH, 45229

Summary

The dentate gyrus is hypothesized to function as a "gate", limiting the flow of excitation through the hippocampus. During epileptogenesis, adult-generated granule cells (DGC) form aberrant neuronal connections with neighboring DGC, disrupting the dentate gate. Hyperactivation of the mTOR signaling pathway is implicated in driving this aberrant circuit formation. While the presence of abnormal DGC in epilepsy has been known for decades, direct evidence linking abnormal DGC to seizures has been lacking. Here, we isolate the effects of abnormal DGC using a transgenic mouse model to selectively delete PTEN from postnatally-generated DGC. PTEN deletion led to hyperactivation of the mTOR pathway, producing abnormal DGC morphologically similar to those in epilepsy. Strikingly, animals in which PTEN was deleted from ≥9% of the DGC population developed spontaneous seizures in about four weeks, confirming that abnormal DGC – which are present in both animals and humans with epilepsy – are capable of causing the disease.

Keywords

phosphatase and tensin homologue; PTEN; mammalian target of rapamycin; mTOR; epileptogenesis; dentate gate; hilar basal dendrite; ectopic dentate granule cell; mossy fiber sprouting; epilepsy

Introduction

Pathological changes within the hippocampal dentate gyrus have long been hypothesized to be a critical step in the development of temporal lobe epilepsy. Per this hypothesis, the

Corresponding author: (Laboratory of Origin), Dr. Steve C. Danzer, 3333 Burnet Avenue, ML 2001, Cincinnati, Ohio 45229-3039, (513) 636-4526 (phone), (513) 636-7337 (fax), steve.danzer@cchmc.org.

The authors have no conflicts of interest to report.

dentate gyrus acts as a gate in the normal brain, limiting the flow of excitatory activity through the hippocampus (Heinemann *et al,.* 1992; Hsu, 2007). During the development of epilepsy, however, this gating function of the dentate is compromised (Behr *et al.*, 1998; Dudek and Sutula; 2007, Pathak *et al.* 2007). The loss of dentate gating is believed to promote the appearance and spread of epileptic seizures. Pathological changes implicated in dysfunction of the dentate include sprouting of granule cell mossy fiber axons into the dentate molecular layer (Tauck and Nadler, 1985; Nadler, 2003), the appearance of ectopic granule cells in the dentate hilus (Scharfman, *et al.*, 2000) and the formation of aberrant basal dendrites by granule cells (Ribak *et al.,* 2000). By creating *de novo* recurrent excitatory circuits within the dentate, these changes can impair the dentate gate.

Pathological integration of dentate granule cells and subsequent disruption of the dentate gate may be a consequence of excess signaling through the mammalian target of rapamycin (mTOR) pathway. The mTOR pathway is activated in several models of epilepsy (Zeng *et al.*, 2009; Huang *et al.,* 2010; Okamoto *et al.,* 2010; Zhang and Wong, 2012) and the mTOR blocker rapamycin has anti-epileptogenic properties (Zeng *et al.*, 2009; Huang *et al.*, 2010) and inhibits mossy fiber sprouting (Buckmaster *et al.*, 2009; Buckmaster and Lew, 2011). Conversely, hyperactivation of the mTOR pathway by deleting phosphatase and tensin homologue (PTEN) is epileptogenic (Backman *et al.*, 2001; Ogawa *et al.*, 2007; Ljungberg et al., 2009). PTEN is a lipid phosphatase which targets the 3′ phosphate of phosphatidylinositol 3,4,5 triphosphate, thus acting in opposition to phosphatidylinositol 3-kinase (PI3K). mTOR is a major target of the PI3K pathway, and deletion of PTEN leads to excess activation of mTOR (Kwon *et al.*, 2003). PTEN knockout granule cells become hypertrophic, migrate to ectopic locations in the hilus and form aberrant basal dendrites (Backman *et al.,* 2001; Kwon *et al.,* 2001; 2003; 2006; Ogawa *et al.,* 2007; Amiri et al., 2012). Therefore, it is reasonable to hypothesize that following an epileptogenic brain injury, excess activation of mTOR among granule cells promotes the formation of abnormal circuits, which in turn destabilize the dentate gate and provoke seizures. To test this hypothesis, we developed a conditional, inducible transgenic mouse model to selectively delete PTEN from a subset of granule cells generated after birth. Deletion was targeted to postnatally-generated neurons, which populate olfactory bulb and dentate gyrus, so the role of the latter structure in epileptogenesis could be largely isolated. If excess mTOR activation among hippocampal dentate granule cells is a plausible mechanism of epileptogenesis, granule cell-specific PTEN knockout mice should become epileptic.

Results

Selective deletion of PTEN from postnatally-generated granule cells

Deletion of PTEN from a subset of postnatally-generated neurons was achieved by treating 14-day-old triple transgenic Gli1-CreER^{T2} hemizygous, PTEN$^{flox/flox}$, GFP reporter$^{+/-}$ (PTEN KO; see figure S1 for breeding strategy) mice with tamoxifen. Effective PTEN deletion was confirmed by simultaneous NeuN and PTEN immunostaining in brain sections from PTEN KO mice (n=30). In these animals, numerous PTEN negative, NeuN-positive neurons were evident in the neurogenic regions of the postnatal brain; the granule cell layer (Fig. 1) and olfactory bulb (Fig. S2). Despite careful analyses of NeuN/PTEN/GFP triple immunostained sagittal sections through the medial-lateral extent of the brain, no other neuronal subtypes exhibited either loss of PTEN or expression of GFP (Fig. S2). In littermate control animals, 100% of NeuN-positive granule cells (2 dentate gyri/mouse, n=23 mice) co-labeled with PTEN antibodies (Fig. 1). Normal patterns of PTEN immunoreactivity were also present in PTEN KO mice that were not treated with tamoxifen (not shown). In addition to neuronal recombination, recombination in non-neuronal cells was evident among astrocytes in midbrain and neocortex (Fig. S3), oligodendrocytes in

corpus callosum (Fig. S3) and Bergmann glial cells in cerebellum (not shown). No animals exhibited gross congenital defects or tumors in the brain.

PTEN deletion reproduces hallmark pathologies of temporal lobe epilepsy

PTEN KO granule cells exhibited numerous morphological abnormalities characteristic of granule cells from rodents with temporal lobe epilepsy (Parent et al., 2006; Jessberger et al., 2007; Walter et al., 2007; Kron et al., 2010; Murphy et al., 2011; Pierce et al., 2011; Murphy et al., 2012), including neuronal hypertrophy, *de novo* appearance of basal dendrites, increased dendritic spine density and ectopically located somata. For illustrative purposes, a small number of PTEN KO animals were crossed into the Thy1-GFP expressing mouse line (Feng et al., 2000; Vuksic et al., 2008; Danzer et al., 2010), which labels a subset of granule cells with GFP regardless of PTEN expression. GFP expression within adjacent wildtype and PTEN KO cells in these animals revealed the dramatic morphological impact of PTEN deletion (Fig. 2, A-B). Quantification of these changes in PTEN KO animals crossed to GFP reporter mice revealed increases in mean soma area from 59.3±3.5 μm^2 in control animals to 176.2±12.1 μm^2 in PTEN KO animals ($p<0.001$, t-test; control n=4 mice [40 cells]; PTEN KO n=5 mice [36 cells]). The percentage of GFP-expressing granule cells ectopically located in the hilus (Fig. 2, F) increased from 0.3±0.3% in controls to 3.3±1.0% in PTEN KO mice ($p=0.049$, t-test; control n=5 mice [519 cells examined]; PTEN KO n=8 mice [1544 cells]). The number of apical dendrites increased from 1 [range 1.0–1.1] in control mice to 1.8 [1.4–2.3] in PTEN KO mice ($p=0.016$, Mann-Whitney rank sum test [RST]; control n=4 [40 cells], PTEN KO n=5 mice [36 cells]). Spine density along these dendrites more than doubled (Fig. 2, C–D), increasing from 2.9±0.4 spines/μm to 7.5±0.5 spines/μm (control, n=4 mice [12 cells]; PTEN KO, n=4 mice [12 cells], $p<0.001$, t-test). The number of basal dendrites/cell increased from an animal median of 0 [range 0–0] in controls to 0.8 [0.4–1.0] in PTEN KO mice (Fig. 3; $p=0.016$, RST; control n=4 mice, [40 cells]; PTEN KO n=5 mice, [36 cells]). Basal dendrites, normally lacking in control rodents, are common in several models of temporal lobe epilepsy. 58.1±6.9% (12 dendrites from 3 mice) of dendritic spines coating these hilar basal dendrites were apposed to puncta immunoreactive for zinc transporter-3 (Fig. 3). Zinc transporter-3 (ZnT-3) labels granule cell mossy fiber terminals (McAuliffe et al., 2011), and the apposition of presynaptic and postsynaptic components implies that PTEN KO cells receive recurrent excitatory input from neighboring granule cells. Further immunostaining experiments revealed the presence of PSD-95 in GFP-expressing basal dendrite spines apposed to ZnT-3 immunoreactive puncta (Fig. 3), supporting the conclusion that these inputs are functional.

PTEN KO mice exhibit spontaneous seizures

Simultaneous video/EEG recordings were made from either hippocampus or cortex of control (n=9) and PTEN KO mice (n=14) using 2-lead wireless EEG transmitters beginning at 6–8 weeks of age. Four additional animals (n=1 control, 3 PTEN KO) were recorded simultaneously from hippocampus and ipsilateral motor cortex using 4-lead wireless transmitters. A total of 96 days of video/EEG data was collected from control animals and 112 days collected from PTEN KO animals. Strikingly, 82% of PTEN KO mice exhibited spontaneous seizures. Two of the three animals that did not exhibit seizures died after only 4 days of recording, so whether they would have exhibited seizures eventually is not known. Many animals exhibited seizures during the first week of recording (≈6–8 weeks of age), indicating that epilepsy can develop in these mice in as little as four weeks after tamoxifen injection. No seizures were observed in any control animals. In PTEN KO animals followed over a period of weeks, the seizure phenotype was progressive. Initially (≈8 weeks), animals exhibited relatively frequent epileptiform activity (e.g. brief spike trains with no change in frequency) and occasional stereotypical seizures, characterized by progressive changes in frequency and amplitude before terminating after about 30–60 seconds (Fig. 4, A). In

animals recorded from hippocampus and cortex simultaneously, epileptiform activity and seizures were consistently observed in hippocampus hours to days before abnormalities were evident in the cortical EEG (Fig. 4, B). Animals were typically immobile during these focal hippocampal seizures. As the animals became older, EEG abnormalities became more severe. Some animals exhibited more frequent stereotypical seizures, which were associated with convulsions when they spread to cortex (Fig. 4, C). Other animals exhibited fewer overt seizures but begin to exhibit increasing amounts of abnormal background activity and interictal spikes. Over time abnormal activity typically devolved to intermittent bursting (Fig. 4, D) or burst suppression patterns (Fig. 4, E), and manifested in both hippocampus and cortex. Latencies between bursts ranged from about 1–60 seconds. Periods of burst suppression could persist for 20–30 minutes or longer, during which animals were largely immobile. Normalization of the EEG in these animals was followed by a return to normal behavior. PTEN KO animals exhibiting burst suppression patterns exhibited poor grooming and declining health. Ten of 17 PTEN KO mice became moribund and were euthanized or died prematurely, compared to only one of ten EEG implanted control mice. Mean age for morbidity/mortality among PTEN KO mice was 2.2 months. Many of these animals exhibited some variation of a burst suppression pattern prior to death. While most of the animals we observed exhibiting this pattern had cortical electrodes only, the animal shown in figure 4, C developed a hippocampal seizure lasting for almost 30 minutes while exhibiting cortical burst suppression. The animal was moribund during this event, raising the possibility that death in some animals might result from underlying non-convulsive status epilepticus.

The extent of CreER^{T2}-mediated recombination varied among PTEN KO animals, so studies were undertaken to determine whether the percentage of granule cells in which PTEN was deleted correlated with epileptogenesis. Among the eight EEG-recorded PTEN KO mice (aged 3–7 months) for which good histology was available (e.g. mice that survived and could be perfusion-fixed), the percentage of dentate granule cells with no detectable PTEN immunoreactivity varied between <1 to 24%. Seizure activity was confirmed in seven of these mice, with PTEN deletion measures of 9–24%. No seizures were observed in the remaining animal which exhibited few PTEN KO granule cells (<1%).

PTEN deletion from olfactory neurons

One limitation of the Gli1 promoter used to target hippocampal granule cell progenitors is that subventricular zone progenitors, which populate olfactory bulb via the rostral migratory stream, are also targeted. Cells produced by this pathway differentiate into inhibitory olfactory granule cells (≈95%; OGCs) or olfactory periglomerular cells (≈5%), the majority of which are also GABAergic (Whitman and Greer, 2009). Although excess growth of inhibitory interneurons may, in principle, be less likely to promote epileptogenesis, it is a formal possibility.

To explore this possibility, we first assessed the morphology of OGCs in olfactory bulb from wildtype and PTEN KO mice (Fig. 5). Initially, GFP expression was used to identify OGCs for morphological characterization in the olfactory bulb. Surprisingly, in olfactory bulb, neither soma area (control, n=5 [77 cells], 41.1±2.2 μm^2; PTEN KO, n=4 [44 cells], 47.2±6.8; p=0.381, t-test) nor primary dendrite number (control, n=5 [77 cells], 3.2±0.2 dendrites/cell; PTEN KO, n=4 [44 cells], 3.7±0.6; p=0.353, t-test) differed between GFP-expressing OGCs in wildtype and PTEN KO mice. Given the robust morphological impact of PTEN deletion from hippocampal granule cells, we queried whether poor recombination efficiency among GFP expressing OGCs might account for this lack of effect. Analysis of PTEN/GFP double immunostaining revealed that only 44.6±6.5% of GFP-expressing OGCs in PTEN KO mice were also immunonegative for PTEN. By contrast, 84±6.1% of GFP-expressing dentate granule cells in PTEN KO mice were PTEN-immunonegative (p=0.007,

t-test). These data suggest that cre recombinase is more effective at inducing GFP expression and deleting PTEN from hippocampal granule cells relative to OGCs, although the mechanism of this phenomenon is not clear. Given these findings, we reexamined OGC soma area in PTEN KO mice, comparing GFP-expressing, PTEN-immunopositive cells to GFP-expressing, PTEN-immunonegative cells. This analysis revealed a clear difference between the two populations, with the latter being significantly larger (GFP+,PTEN+, 37.5±2.1 μm^2; GFP+,PTEN−, 65.4±4.5; $p<0.001$, t-test). Interestingly, the 75% increase in OGC soma area was less than half the almost 200% increase observed among hippocampal granule cells, suggesting that the hippocampal granule cells may respond more robustly to PTEN deletion.

To confirm that olfactory bulb was not the source of the seizure activity in PTEN KO mice, dual EEG recordings were made from olfactory bulb and hippocampus of four PTEN KO animals. In these animals, numerous episodes of epileptiform activity and seizures were observed in hippocampal EEG traces. During these events, EEG traces from olfactory bulb were qualitatively normal (Fig. 5). No examples of seizure activity originating in olfactory bulb and spreading to hippocampus were observed during four weeks of continuous video/EEG monitoring. These findings strongly suggest that olfactory bulb is not driving seizure activity in these animals, and support the conclusion that hippocampus is the source of the seizures.

PTEN KO mice exhibit minimal reactive gliosis

Deletion of the mTOR inhibitor Tsc1 primarily from astrocytes leads to the development of epilepsy in mice(Uhlmann et al., 2002; Erbayat-Altay et al., 2007). The mechanism underlying epileptogenesis in this model is still being explored; however, a recent study suggests that decreased expression and function of astrocyte glutamate transporters may be important (Zeng et al., 2010). Glial changes are also implicated in other animal models of epilepsy as well as humans with the condition (for review see Vezzani et al., 2011). We queried, therefore, whether astrocytic changes might be an important feature in PTEN KO animals by staining brain sections from wildtype and PTEN KO mice with the astrocytic marker GFAP. Hippocampi from five wildtype and five PTEN KO animals were examined, with the latter exhibiting PTEN deletion from 14–24% of the granule cell population. While a couple PTEN KO animals showed some evidence of reactive astrocytosis, such as enlarged glial cell bodies, thicker astrocytic processes and brighter GFAP labeling (Fig. S4), quantitative measures of astrocyte cell body area (based on GFAP labeling) did not reveal a significant difference between groups (wildtype, 36.7±4.3 μm^2; PTEN KO, 51.6±6.2 μm^2; $p=0.085$, t-test). Similarly, no difference was observed in the density of labeled astrocytes (wildtype, 49.5±11.6 astrocytes × $10^3 mm^{-3}$; PTEN KO, 46.8±14.0 × $10^3 mm^{-3}$; $p=0.886$, t-test), with values being roughly similar to published reports for C57BL/6 mice (Ogata and Kosaka, 2002).

The lack of a glial phenotype in PTEN KO animals likely reflects the low recombination rates among these cells. GFP-expressing astrocytes were virtually absent from hippocampus (on average 5.7±3.1 astrocytes/hippocampus; n=6 PTEN KO animals) and were rare throughout cortex (Fig. S3; 0.8±0.4% of glial cells expressed GFP, n=3 PTEN KO mice). Quantification of the number of GFP-expressing astrocytes in the lateral posterior thalamic nucleus, a region showing comparatively large numbers of recombined astrocytes (Fig. S3, boxed region), produced only slightly larger recombination rates (2.7±0.8%, n=3 PTEN KO mice). Finally, in contrast to neurons, in which PTEN immunoreactivity was readily detectable in wildtype cells and clearly absent in knockout cells (Fig. 1), PTEN immunoreactivity was undetectable among GFP-expressing (recombined) astrocytes from both wildtype and KO animals (Fig. S4). Comparatively low levels of endogenous PTEN

protein in this astrocyte population lead us to speculate that PTEN deletion from these cells may have relatively minimal effects.

Epileptogenesis in PTEN KO mice is mediated by enhanced mTOR activation

PTEN deletion is predicted to lead to increased phosphorylation of the mTOR effector S6. To determine whether the mTOR pathway was disrupted in PTEN KO mice, sections from six control and nine PTEN KO mice were immunostained for phospho-S6 (pS6). pS6 immunostaining intensity was significantly higher within the dentate gyrus of PTEN KO mice relative to controls (control, 77% [25–171] over background; PTEN KO, 160% [105–526] over background; p=0.022, RST), consistent with previous studies (Amiri et al., 2012). These findings are indicative of enhanced mTOR signaling in these animals.

To confirm that the seizure phenotype was mediated by the mTOR pathway, PTEN KO animals were treated with the mTOR antagonist rapamycin. Rapamycin treatment significantly reduced seizure frequency in PTEN KO animals (n=5) relative to vehicle treated PTEN KO animals (n=4). Specifically, 100% of vehicle-treated PTEN KO animals developed epilepsy, with a median seizure frequency of 0.69/day (range: 0.40 – 2.60). Only 2 of 5 rapamycin treated KO mice exhibited any seizures at all, leading to an overall median seizure frequency of 0.06/day (range: 0.00 – 0.17; p=0.016, RST). These findings likely underestimate the effect of rapamycin on seizures in this model, as rapamycin also reduced the growth rate of treated mice, making it necessary to delay electrode implantation until animals reached criterion weight (18–20g) for implantation of wireless EEG devices. Vehicle-treated PTEN KOs reached 18g at a mean age of 8.3 ± 0.5 weeks, while rapamycin-treated KOs didn't reach this weight until they were 13.8 ± 1.2 weeks-old. Advantageously, rapamycin also appeared to mitigate progression in this model and prolonged animal survival, so despite the greater age of rapamycin-treated PTEN KOs during EEG recording, they still exhibited fewer seizures than their younger vehicle-treated PTEN KO siblings.

The number of granule cells immunoreactive for pS6 was significantly reduced in PTEN KO animals treated with rapamycin relative to vehicle treated KOs (Fig. 6, vehicle, 17.5 [15–35] cells/field; rapamycin 1 [0–14]; p=0.029, RST), confirming the efficacy of the drug. None of the rapamycin treated PTEN KOs exhibited mossy fiber axon sprouting in the inner molecular layer, while all 4 vehicle treated KOs had obvious mossy fiber sprouting (Fig. 6). Taken together, these finding strongly implicate excess activation of the mTOR pathway in mediating epileptogenesis and granule cell pathology in these animals.

Neuronal hypertrophy precedes and mossy fiber sprouting follows epileptogenesis in PTEN knockouts

Mossy fiber sprouting occurs when granule cell axons sprout into the dentate inner molecular layer and form excitatory synaptic connections with other granule cells. The creation of these recurrent excitatory circuits is hypothesized to be a contributing factor in the development of temporal lobe epilepsy (Sutula and Dudek, 2007). To assess mossy fiber sprouting among PTEN KO animals, brain sections were immunostained for ZnT-3. A significant positive correlation was found between the percentage of PTEN KO granule cells in the dentate and the extent of mossy fiber sprouting in the inner molecular layer (Fig. 7; R=0.757, p=0.007, Pearson product moment correlation). Essentially, mice with >16% PTEN KO granule cells (n=5) exhibited robust mossy fiber sprouting (Fig. 7) and exhibited spontaneous seizures. By contrast, animals with PTEN deletions from <15% of their granule cells populations exhibited no mossy fiber sprouting. Interestingly, three of these animals with 9–15% recombination rates were confirmed as epileptic by video/EEG monitoring. This implies that mossy fiber sprouting is not required for epileptogenesis in this model. Granule cell soma area, on the other hand, was dramatically increased in all PTEN KO

animals examined, regardless of whether they had seizures (Fig. 7). These cells also possessed basal dendrites (not shown). Taken together, these finding suggest the neuronal hypertrophy may be important for epileptogenesis in this model, while mossy fiber sprouting may be a consequence of recurrent seizures rather than a cause.

Wildtype granule cells contribute to mossy fiber sprouting in PTEN KO mice

Three animals with robust mossy fiber sprouting were selected to determine the relative contribution of PTEN KO cells to this phenomenon. Mossy fiber terminals in the inner molecular layer were identified by ZnT-3 immunolabeling, and the percentage of these terminals co-labeled with GFP was determined. In these animals, 25.2±2.3% of ZnT-3 immunoreactive puncta in the inner molecular layer were GFP positive (Fig. 8), indicating that about a quarter of the mossy fiber sprouting is due to PTEN KO cells. This corresponded roughly to the total number of PTEN KO cells in these animals, at 20.9±2.0%.

Discussion

A long-standing hypothesis in the epilepsy field postulates that aberrant granule cells can cause temporal lobe epilepsy, but direct evidence in support of this idea has been limited. To test this hypothesis, we used a conditional, inducible transgenic mouse model to selectively eliminate PTEN gene expression from neural progenitor cells beginning 14 days after birth. This led PTEN KO hippocampal granule cells to integrate abnormally into the hippocampus, recapitulating pathologies common in models of temporal lobe epilepsy. Supporting the hypothesized role of abnormal granule cells in temporal lobe epileptogenesis, animals in which PTEN was deleted from as little as 9% of the hippocampal granule cell population developed epilepsy. Since limited recombination also occurred among cortical astrocytes and olfactory granule cells, morphological and EEG studies of these regions were also conducted. The morphological impact of PTEN deletion among these cells was much less robust than hippocampal granule cells, and dual EEG recording experiments allowed us to exclude cortex and olfactory bulb as the source of seizures. Together, these studies provide new evidence in support of the hypothesis that abnormal granule cells can mediate epileptogenesis.

Source of epileptogenesis in PTEN KO mice

A key conclusion of the present study is that PTEN deletion among hippocampal granule cells is sufficient to cause epilepsy. It is worth considering, therefore, the evidence implicating these cells in PTEN KO animals. To start, we note that no tumors were observed in these animals, consistent with previous studies indicating that PTEN deletion, by itself, is not necessarily tumorigenic (Backman *et al.,* 2001; Kwon *et al.,* 2001; 2003; 2006; Fraser *et al.*, 2004; 2008; Ogawa *et al.,* 2007; Gregorian *et al.,* 2009). There is no evidence, therefore, that neoplastic lesions are responsible for the epilepsy phenotype in the animals described here.

Seizures do not appear to be driven by recombined cortical glial cells. The Gli1-CreER^{T2} transgenic system led to the selective deletion of PTEN from a small number of glial cells; mostly protoplasmic astrocytes. Recombined (GFP-expressing) astrocytes were present in many brain regions, but made up only a few percent or less of total glial cells. Enhanced mTOR signaling in glial cells is hypothesized to drive epileptogenesis in conditional GFAP-Cre::Tsc1$^{fl/fl}$ mice (Zeng et al., 2008; Zeng et al., 2010), however, in these animals Tsc1 is eliminated from >90% of astrocytes (Bajenaru et al., 2002) as well as some neurons (Su et al., 2004), so the pattern of PTEN deletion in these mice is very different from the present study. Moreover, overt changes in astrocyte morphology were absent in PTEN KO animals, suggesting that these cells are minimally affected by PTEN deletion (relative to granule

cells). The Gli1 promoter drives cre recombinase expression in non-proliferating mature astrocytes (Garcia et al., 2010). Therefore, in contrast to granule cells, in which PTEN is deleted prior to neuronal maturation, deletion of PTEN after astrocytes have already matured may minimize the effects of gene loss. In addition, while PTEN protein was readily detectable among control neurons, we were unable to detect PTEN protein among control astrocytes, indicating that the protein is either below detection thresholds or is absent from the population examined. Finally, despite the presence of small numbers of recombined glia in cortex, dual cortical-hippocampal EEG recording demonstrated that seizures appear first in hippocampus without cortical involvement, implicating the former structure as the source of the seizures.

Seizures do not appear to be driven by olfactory neurons. Gli1-CreER^{T2} is expressed in subventricular zone progenitors, which produce neuroblasts and immature neurons that migrate to the olfactory bulb via the rostral migratory stream. Upon arrival in the olfactory bulb, the majority of these cells differentiate into GABAergic olfactory granule cells, while a minority (≈5%) becomes periglomerular cells (Whitman and Greer, 2009). The processes of these cells are restricted to the olfactory bulb, where they modulate the activity of mitral and tufted cells. The inhibitory phenotype of affected cells, and a paucity of data linking the olfactory bulb to epileptogenesis, makes these neurons unlikely candidates for producing the seizure phenotype exhibited by PTEN KO mice. Several additional lines of evidence support this conclusion. Firstly, mice in which PTEN was selectively deleted from olfactory bulb, but not hippocampus, appeared neurologically normal (although seizure activity was not assessed) and survived for up to two years in previous studies (Gregorian *et al.,* 2009). By contrast, PTEN deletion using Cre-driver mouse lines that include dentate granule cells among their targets consistently produce a seizure-phenotype and premature death (Backman *et al.,* 2001; Fraser *et al.,* 2004; Ogawa *et al.,* 2007; Zhou *et al.,* 2009). Secondly, the effects of PTEN deletion on olfactory neuron morphology were relatively modest compared to hippocampal granule cells. Finally, simultaneous EEG recordings from hippocampus and olfactory bulb revealed that seizure activity can occur in hippocampus in these animals with no olfactory bulb involvement.

The prominent abnormalities exhibited by hippocampal granule cells, the predicted excitatory nature of these abnormalities, the localization of seizures to hippocampus and the comparatively modest effect of PTEN deletion on other cell types strongly favors PTEN KO granule cells as the source of the seizures. The possibility that PTEN KO cells in other brain regions play some role cannot be entirely excluded. Nonetheless, a pivotal role for PTEN KO hippocampal granule cells is clearly the most parsimonious explanation. Additional studies, perhaps using even more specific gene knockout strategies, may yield more insights in the future.

Percentage of abnormal granule cells required for epileptogenesis

Epileptogenesis in the present study required surprisingly few PTEN KO granule cells (9–25% of the entire population). Intriguingly, however, key granule cell pathologies in other models of temporal lobe epilepsy also appear to be restricted to a subset of dentate granule cells. Recent studies demonstrate that basal dendrites, hilar ectopic cells and mossy fiber sprouting all result from disruption of newly-generated granule cells. Granule cells already mature at the time of an epileptogenic insult do not participate (Parent *et al.*, 2006; Walter *et al.*, 2007; Kron *et al.*, 2010; Santos et al., 2011; Danzer, 2012). Gli1-CreER^{T2} expression in the neonatal dentate gyrus is restricted to granule cell progenitors, so PTEN deletion in the present study targets that same population of neurons that is implicated in these traditional models of temporal lobe epilepsy. While small in relative number, however, computational modeling studies predict that only 5% of the granule cell population needs to be abnormal to

support seizures (Morgan and Soltesz, 2008). It is notable, therefore, that abnormal granule cell numbers here were well above this threshold, and epilepsy developed rapidly.

Mechanism of epileptogenesis in PTEN KO mice

PTEN deletion reproduced numerous hippocampal granule cell pathologies associated with temporal lobe epilepsy, including mossy fiber sprouting (Tauck and Nadler, 1985; Nadler, 2003), ectopic granule cells (Scharfman *et al.*, 2000), hilar basal dendrites (Ribak *et al.,* 2000), somatic hypertrophy and increased spine density (Murphy et al., 2011). Mossy fiber sprouting was only present among a subset of PTEN KO animals with seizures; however, sprouting was strongly correlated with the percentage of PTEN KO cells within the dentate. Taken together, these observations indicate that sprouting is not required for epilepsy in this model, but that greater numbers of KO cells promote more robust sprouting. Moreover, in animals with robust sprouting, roughly 75% was derived from GFP-negative (PTEN wildtype) cells (Fig. 8). One plausible interpretation of these findings is that animals with more KO cells develop a more severe or earlier onset epilepsy. Repeated seizures can induce mossy fiber sprouting among wildtype granule cells (Cavazos et al., 1991), so earlier disease onset or more severe disease would be predicted to promote greater mossy fiber sprouting. Technical limitations in recording 24/7 EEG from very young animals precluded us from determining the age at which seizures first appear in these animals, and analysis of data from older animals did not reveal any significant correlations. Nevertheless, the ability to dissociate mossy fiber sprouting and seizures could make this a useful model for future studies of this particular plasticity.

In contrast to mossy fiber sprouting, neuronal hypertrophy, basal dendrites and increases in spine density were present among almost all PTEN KO granule cells regardless of whether the animals developed epilepsy, indicating that these changes could contribute to disease etiology. Recent work suggests that neuronal hypertrophy and increased spine density observed here likely reflect pro-excitatory changes in granule cells (Luikart et al., 2011). In this prior study, PTEN mRNA was targeted in granule cells using a shRNA-lentiviral approach, reducing PTEN levels by about 80%. While increases in soma area and spine density were much more modest than those observed here following gene deletion, electrophysiological studies of the knockdown cells revealed an enhancement of excitatory drive. The even larger increases in spine density in the present study may reflect even greater increases in synaptic input. Similarly, basal dendrites support the formation of recurrent excitatory circuits among granule cells in traditional models of epilepsy (Austin and Buckmaster, 2004; Pierce *et al.*, 2005; Sutula and Dudek, 2007; Cameron *et al.*, 2011). The present finding that >50% of spines along granule cell basal dendrites were apposed to granule cell presynaptic terminals suggests that PTEN KO cells also support recurrent circuits. While it is tempting to speculate that these changes mediate epileptogenesis in this model, however, future studies will be required to fully address this issue. The impact of PTEN deletion on granule cell function is likely widespread, and could impact many aspects of cell function not examined here.

Summary

It remains uncertain whether excess mTOR activation among immature granule cells, and subsequent abnormal integration of these cells, accounts for the development of temporal lobe epilepsy. The present findings, however, demonstrate that such a mechanism *is capable of causing the disease*. This observation, combined with previous demonstrations that the mTOR pathway is activated during epileptogenesis, that mTOR blockers can inhibit epileptogenesis, and the almost ubiquitous presence of abnormal granule cells in both animals and humans with temporal lobe epilepsy, indicates that this is a plausible disease mechanism.

Experimental Procedures

Gli1-CreER^{T2}-expressing mice (Ahn and Joyner, 2004; 2005) were used to drive cre-recombinase expression in neural progenitor cells. These animals were crossed to Pten^{tm1Hwu}/J mice (Jackson Laboratory), which possess loxP sites ("floxed") on either side of exon 5 of the PTEN gene, and CAG-CAT-EGFP (GFP reporter) mice (Nakamura *et al.*, 2006). Treatment of triple transgenic mice with tamoxifen, to activate cre-recombinase, leads to PTEN deletion and GFP expression among Gli1 expressing neural progenitors and all subsequent progeny. Mice were maintained on a C57BL/6 background. The following genotypes were used for study:

1. Gli1-CreER^{T2} negative, PTEN$^{wt/wt}$, GFP$^{+/-}$ or GFP$^{-/-}$ [wt control, n=4]
2. Gli1-CreER^{T2} negative, PTEN$^{flox/flox}$, GFP$^{+/-}$ or GFP$^{-/-}$ [flox control, n=13]
3. Gli1-CreER^{T2} hemizygous, PTEN$^{wt/wt}$, GFP$^{+/-}$ or GFP$^{-/-}$ [cre control, n=22]
4. Gli1-CreER^{T2} hemizygous, PTEN$^{flox/flox}$, GFP$^{+/-}$ or GFP$^{-/-}$ [PTEN KO, n=42]

All mice were injected with tamoxifen (2 mg dissolved in 0.2 ml corn oil) subcutaneously at two-weeks-of-age. At this age, the only Gli1-expressing neural progenitor cells still active in the CNS are subgranular zone progenitors, which produce dentate granule cells, and subventricular zone progenitors, which produce olfactory neurons (Bayer SA, 1980a; 1980b; Ming and Song, 2005). At approximately six weeks, mice were implanted with cortical surface electrodes or hippocampal depth electrodes connected to wireless EEG transmitters placed under the skin of the back (TA11ETAF10, Data Sciences International, St. Paul, MN). A subset of animals was implanted with 4-lead transmitters, for simultaneous monitoring of hippocampus and cortex, or hippocampus and olfactory bulb. Animals were monitored 24/7 by video/EEG for up to two months. Video-EEG data was reviewed by a clinically trained epileptologist (KDH) using Neuroscore software (Version 2.1.0, Data Sciences International) to identify seizures. EEG events scored as seizures were characterized by the sudden onset of high amplitude (>2X background) activity, signal progression (a change in amplitude and frequency over the course of the event) and a duration greater than ten seconds.

Rapamycin Treatments

PTEN KO mice (n = 9), induced with tamoxifen at P14, were injected intraperitoneally with either rapamycin (6 mg/kg body weight; n = 5) or vehicle (n = 4) once per day for five consecutive days per week (Monday to Friday) beginning 2–5 days post tamoxifen injection. The initial littermate-controlled rapamycin and vehicle pair of mice was injected weekly; however, due to the reduced growth rate of rapamycin treated mice, subsequent littermate pairs were injected on an alternating week-on/week-off schedule (Sunnen et al., 2011). Upon reaching a weight of 18 g, mice were implanted with cortical electrodes as described above. Animals were monitored 24/7 by video/EEG for at least 10 days.

Histological analyses

At the completion of recording experiments, animals were perfusion fixed, brains sectioned and processed for histological studies. Histological studies were conducted on animals aged 2–7 months, with control and PTEN KO animals being matched for age and brain region (Paxinos and Franklin, 2001) for each parameter assessed. Sections were triple-immunostained against GFP+NeuN+PTEN to determine the percentage of PTEN KO hippocampal granule cells in each animal. Percentages were determined from three-dimensional confocal "image stacks" through the z-depth of the tissue (Leica SP5 confocal system) using Neurolucida software. Sections immunostained for GFP and ZnT-3 were used to assess mossy fiber sprouting. Triple-immunostaining for GFP, ZnT-3 and PSD-95 was

used to examine mossy fiber innervation of basal dendrites. Immunostaining for GFP and GFAP were used to assess tissue for glial changes and reactive gliosis. Cell densities were determined using a variation of the optical dissector method (Howell et al., 2002). Immunostaining for the phosphorylated form of S6 (pS6) was used to assess activation of the mTOR pathway. GFP immunostained sections were also used to assess granule cell soma area, spine density and dendrite number.

Statistics and data analysis

For all analyses, statistical significance was determined using Sigma Plot software (version 12.0, Systat Software, Inc., San Jose, CA). Parametric tests were used for data that met assumptions of normality and equal variance, and non-parametric equivalents were used for data that did not meet these assumptions. Specific tests were used as noted in the results. All t-tests were two-tailed. Data are presented as means±standard error or medians [range].

Supplementary Material

Refer to Web version on PubMed Central for supplementary material.

Acknowledgments

This work was supported by the Cincinnati Children's Hospital Research Foundation and the National Institute of Neurological Disorders and Stroke (SCD, Award Numbers R01NS065020 and R01NS062806). The content is solely the responsibility of the authors and does not necessarily represent the official views of the National Institute of Neurological Disorders and Stroke or the National Institutes of Health. We would like to thank Keri Kaeding for useful comments on earlier versions of this manuscript.

References

Ahn S, Joyner AL. Dynamic changes in the response of cells to positive hedgehog signaling during mouse limb patterning. Cell. 2004; 118:505–516. [PubMed: 15315762]

Ahn S, Joyner AL. *In vivo* analysis of quiescent adult neural stem cells responding to Sonic hedgehog. Nature. 2005; 437:894–897. [PubMed: 16208373]

Austin JE, Buckmaster PS. Recurrent excitation of granule cells with basal dendrites and low interneuron density and inhibitory postsynaptic current frequency in the dentate gyrus of macaque monkeys. J Comp Neurol. 2004; 476(3):205–18. [PubMed: 15269966]

Amiri A, Cho W, Zhou J, Birnbaum SG, Sinton CM, McKay RM, Parada LF. Pten Deletion in Adult Hippocampal Neural Stem/Progenitor Cells Causes Cellular Abnormalities and Alters Neurogenesis. J Neurosci. 2012; 32:5880–5890. [PubMed: 22539849]

Backman SA, Stambolic V, Suzuki A, Haight J, Elia A, Pretorius J, Tsao MS, Shannon P, Bolon B, Ivy GO, Mak TW. Deletion of Pten in mouse brain causes seizures, ataxia and defects in soma size resembling Lhermitte-Duclos disease. Nat Genet. 2001; 29:396–403. [PubMed: 11726926]

Bajenaru ML, Zhu Y, Hedrick NM, Donahoe J, Parada LF, Gutmann DH. Astrocyte-specific inactivation of the neurofibromatosis 1 gene (NF1) is insufficient for astrocytoma formation. Mol Cell Biol. 2002; 22(14):5100–13. [PubMed: 12077339]

Bayer SA. Development of the hippocampal region in the rat. I. Neurogenesis examined with 3H-thymidine autoradiography. J Comp Neurol. 1980a; 190:87–114. [PubMed: 7381056]

Bayer SA. Development of the hippocampal region in the rat. II. Morphogenesis during embryonic and early postnatal life. J Comp Neurol. 1980b; 190:115–134. [PubMed: 7381049]

Behr J, Lyson KJ, Mody I. Enhanced propagation of epileptiform activity through the kindled dentate gyrus. J Neurophysiol. 1998; 79:1726–1732. [PubMed: 9535942]

Buckmaster PS, Ingram EA, Wen X. Inhibition of the mammalian target of rampamycin signaling pathway suppresses dentate granule cell axon sprouting in a rodent model of temporal lobe epilepsy. J Neurosci. 2009; 29:8259–8269. [PubMed: 19553465]

Buckmaster PS, Lew FH. Rapamycin suppresses mossy fiber sprouting but not seizure frequency in a mouse model of temporal lobe epilepsy. J Neurosci. 2011; 31(6):2337–47. [PubMed: 21307269]

Cameron MC, Zhan RZ, Nadler JV. Morphologic integration of hilar ectopic granule cells into dentate gyrus circuitry in the pilocarpine model of temporal lobe epilepsy. J Comp Neurol. 2011; 519(11): 2175–92. [PubMed: 21455997]

Cavazos JE, Golarai G, Sutula TP. Mossy fiber synaptic reorganization induced by kindling: time course of development, progression, and permanence. J Neurosci. 1991; 11(9):2795–803. [PubMed: 1880549]

Danzer SC, He XP, Loepke AW, McNamara JO. Structural plasticity of dentate granule cell presynaptic terminals during the development of limbic epilepsy. Hippocampus. 2010; 20:113–124. [PubMed: 19294647]

Danzer SC. Depression, stress, epilepsy and adult neurogenesis. Experimental Neurology. 2012; 233(1):22–32. [PubMed: 21684275]

Dudek FE, Sutula TP. Epileptogenesis in the dentate gyrus: a critical perspective. Prog Brain Res. 2007; 163:755–773. [PubMed: 17765749]

Erbayat-Altay E, Zeng LH, Xu L, Gutmann DH, Wong M. The natural history and treatment of epilepsy in a murine model of tuberous sclerosis. Epilepsia. 2007; 48(8):1470–6. [PubMed: 17484760]

Feng G, Mellor RH, Bernstein M, Keller-Peck C, Nguyen QT, Wallace M, Nerbonne JM, Lichtman JW, Sanes JR. Imaging neuronal subsets in transgenic mice expressing multiple spectral variants of GFP. Neuron. 2000; 28:41–51. [PubMed: 11086982]

Fraser MM, Zhu X, Kwon CH, Uhlmann EJ, Gutmann DH, Baker SJ. *Pten* loss causes hypertrophy and increased proliferation of astrocytes in vivo. Cancer Res. 2004; 64:7773–7779. [PubMed: 15520182]

Fraser MM, Bayazitov IT, Zakharenko SS, Baker SJ. Phosphatase and tensin homolog, deleted on chromosome 10 deficiency in brain causes defects in synaptic structure, transmission and plasticity, and myelination abnormalities. Neuroscience. 2008; 151:476–488. [PubMed: 18082964]

Garcia AD, Petrova R, Eng L, Joyner AL. Sonic hedgehog regulates discrete populations of astrocytes in the adult mouse forebrain. J Neurosci. 2010; 30(41):13597–608. [PubMed: 20943901]

Gregorian C, Nakashima J, Le Belle J, Ohab J, Kim R, Liu A, Smith KB, Groszer M, Garcia AD, Sofroniew MV, Carmichael ST, Kornblum HI, Liu S, Wu H. *Pten* deletion in adult neural stem/progenitor cells enhances constitutive neurogenesis. J Neurosci. 2009; 29:1874–1886. [PubMed: 19211894]

Heinemann U, Beck H, Dreier JP, Ficker E, Stabel J, Zhang CL. The dentate gyrus as a regulated gate for the propagation of epileptiform activity. Epilepsy Res Suppl. 1992; 7:273–280. [PubMed: 1334666]

Howell K, Hopkins N, Mcloughlin P. Combined confocal microscopy and stereology: a highly efficient and unbiased approach to quantitative structural measurement in tissues. Exp Physiol. 2002; 87:747–756. [PubMed: 12530405]

Hsu D. The dentate gyrus as a filter or gate: a look back and a look ahead. Prog Brain Res. 2007; 163:601–613. [PubMed: 17765740]

Huang X, Zhang H, Yang J, Wu J, McMahon J, Lin Y, Cao Z, Gruenthal M, Huang Y. Pharmacological inhibition of the mammalian target of rapamycin pathway suppresses acquired epilepsy. Neurobiol Dis. 2010; 40:193–199. [PubMed: 20566381]

Jessberger S, Zhao CM, Toni N, Clemenson GD Jr, Li Y, Gage FH. Seizure-associated, aberrant neurogenesis in adult rats characterized with retrovirus-mediated cell labeling. J Neurosci. 2007; 27:9400–9407. [PubMed: 17728453]

Kron MM, Zhang H, Parent JM. The developmental stage of dentate granule cells dictates their contribution to seizure-induced plasticity. J Neurosci. 2010; 30:2051–2059. [PubMed: 20147533]

Kwon CH, Zhu X, Zhang J, Knoop LL, Tharp R, Smeyne RJ, Eberhart CG, Burger PC, Baker SJ. *Pten* regulates neuronal soma size: a mouse model of Lhermitte-Duclos disease. Nat Genet. 2001; 29:404–411. [PubMed: 11726927]

Kwon CH, Zhu X, Zhang J, Baker SJ. mTor is required for hypertrophy of *Pten*-deficient neuronal soma *in vivo*. Proc Natl Acad Sci (USA). 2003; 100:12923–12928. [PubMed: 14534328]

Kwon CH, Luikart BW, Powell CM, Zhou J, Matheny SA, Zhang W, Li Y, Baker SJ, Parada LF. Pten regulates neuronal arborization and social interaction in mice. Neuron. 2006; 50:377–388. [PubMed: 16675393]

Ljungberg MC, Sunnen CN, Lugo JN, Anderson AE, D'Arcangelo G. Rapamycin suppresses seizures and neuronal hypertrophy in a mouse model of cortical dysplasia. Dis Model Mech. 2009; 2(7–8): 389–98. [PubMed: 19470613]

Luikart BW, Schnell E, Washburn EK, Bensen AL, Tovar KR, Westbrook GL. *Pten* knockdown *in vivo* increases excitatory drive onto dentate granule cells. J Neurosci. 2011; 31:4345–4354. [PubMed: 21411674]

McAuliffe JJ, Bronson SL, Hester MS, Murphy BL, Dahlquist-Topalá R, Richards DA, Danzer SC. Altered patterning of dentate granule cell mossy fiber inputs onto CA3 pyramidal cells in limbic epilepsy. Hippocampus. 2011; 21(1):93–107. [PubMed: 20014385]

Ming GL, Song H. Adult neurogenesis in the mammalian central nervous system. Ann Rev Neurosci. 2005; 28:223–250. [PubMed: 16022595]

Morgan RJ, Soltesz I. Nonrandom connectivity of the epileptic dentate gyrus predicts a major role for neuronal hubs in seizures. Proc Natl Acad Sci (USA). 2008; 105:6179–6184. [PubMed: 18375756]

Murphy BL, Pun RYK, Yin H, Faulkner CR, Loepke AW, Danzer SC. Heterogeneous integration of adult-generated granule cells into the epileptic brain. J Neurosci. 2011; 31:105–117. [PubMed: 21209195]

Murphy BL, Hofacer RD, Faulkner CN, Loepke AW, Danzer SC. Abnormalities of granule cell dendritic structure are a prominent feature of the intrahippocampal kainic acid model of epilepsy despite reduced postinjury neurogenesis. Epilepsia. 2012; 53(5):908–21. [PubMed: 22533643]

Nadler JV. The recurrent mossy fiber pathway of the epileptic brain. Neurochem Res. 2003; 28:1649–1658. [PubMed: 14584819]

Nakamura T, Colbert MC, Robbins J. Neural crest cells retain multipotential characteristics in the developing valves and label the cardiac conduction system. Circ Res. 2006; 98:1547–1554. [PubMed: 16709902]

Ogata K, Kosaka T. Structural and quantitative analysis of astrocytes in the mouse hippocampus. Neuroscience. 2002; 113(1):221–33. [PubMed: 12123700]

Ogawa S, Kwon CH, Zhou J, Koovakkattu D, Parada LF, Sinton CM. A seizure-prone phenotype is associated with altered free-running rhythm in *Pten* mutant mice. Brain Res. 2007; 1168:112–123. [PubMed: 17706614]

Okamoto OK, Janjoppi L, Bonone FM, Pansani AP, Da Silva AV, Scorza FA, Cavalheiro EA. Whole transcriptome analysis of the hippocampus: toward a molecular portrait of epileptogenesis. BMC Genomics. 2010; 11:230. [PubMed: 20377889]

Parent JM, Elliott RC, Pleasure SJ, Barbaro NM, Lowenstein DH. Aberrant seizure-induced neurogenesis in experimental temporal lobe epilepsy. Ann Neurol. 2006; 59:81–91. [PubMed: 16261566]

Pathak HR, Weissinger F, Terunuma M, Carlson GC, Hsu FC, Moss SJ, Coulter DA. Disrupted dentate granule cell chloride regulation enhances synaptic excitability during development of temporal lobe epilepsy. J Neurosci. 2007; 27:14012–14022. [PubMed: 18094240]

Paxinos, G.; Franklin, KBJ. The Mouse Brain in Stereotaxic Coordinates. Academic Press; San Diego: 2001.

Pierce JP, Melton J, Punsoni M, McCloskey DP, Scharfman HE. Mossy fibers are the primary source of afferent input to ectopic granule cells that are born after pilocarpine-induced seizures. Exp Neurol. 2005; 196(2):316–31. [PubMed: 16342370]

Pierce JP, McCloskey DP, Scharfman HE. Morphometry of hilar ectopic granule cells in the rat. J Comp Neurol. 2011; 519(6):1196–218. [PubMed: 21344409]

Ribak CE, Tran PH, Spigelman I, Okazaki MM, Nadler JV. Status epilepticus-induced hilar basal dendrites on rodent granule cells contribute to recurrent excitatory circuitry. J Comp Neurol. 2000; 428:240–253. [PubMed: 11064364]

Santos VR, Wagner de Castro O, Pun RYK, Hester MS, Murphy BL, Loepke AW, Garcia-Cairasco N, Danzer SC. Contributions of mature granule cells to structural plasticity in temporal lobe epilepsy. Neuroscience. 2011; 197:348–57. [PubMed: 21963349]

Scharfman HE, Goodman JH, Sollas AL. Granule-like neurons at the hilar/CA3 border after status epilepticus and their synchrony with area CA3 pyramidal cells: functional implications of seizure-induced neurogenesis. J Neurosci. 2000; 20:6144–6158. [PubMed: 10934264]

Su M, Hu H, Lee Y, d'Azzo A, Messing A, Brenner M. Expression specificity of GFAP transgenes. Neurochem Res. 2004; 29(11):2075–93. [PubMed: 15662842]

Sunnen CN, Brewster AL, Lugo JN, Vanegas F, Turcios E, Mukhi S, Parghi D, D'Arcangelo G, Anderson AE. Inhibition of the mammalian target of rapamycin blocks epilepsy progression in NS-Pten conditional knockout mice. Epilepsia. 2011; 52(11):2065–75. [PubMed: 21973019]

Sutula TP, Dudek FE. Unmasking recurrent excitation generated by mossy fiber sprouting in the epileptic dentate gyrus: an emergent property of a complex system. Prog Brain Res. 2007; 163:541–63. [PubMed: 17765737]

Tauck DL, Nadler JV. Evidence of functional mossy fiber sprouting in hippocampal formation of kainic acid-treated rats. J Neurosci. 1985; 5:1016–1022. [PubMed: 3981241]

Uhlmann EJ, Wong M, Baldwin RL, Bajenaru ML, Onda H, Kwiatkowski DJ, Yamada K, Gutmann DH. Astrocyte-specific TSC1 conditional knockout mice exhibit abnormal neuronal organization and seizures. Ann Neurol. 2002; 52(3):285–96. [PubMed: 12205640]

Vezzani A, Aronica E, Mazarati A, Pittman QJ. Epilepsy and brain inflammation. Exp Neurol. 2011 Oct 1.2011 [Epub ahead of print].

Vuksic M, Del Turco D, Bas Orth C, Burbach GJ, Feng G, Müller CM, Schwarzacher SW, Deller T. 3D-reconstruction and functional properties of GFP-positive and GFP-negative granule cells in the fascia dentata of the Thy1-GFP mouse. Hippocampus. 2008; 18:364–75. [PubMed: 18189310]

Walter C, Murphy BL, Pun RY, Spieles-Engemann AL, Danzer SC. Pilocarpine-induced seizures cause selective time-dependent changes to adult-generated hippocampal dentate granule cells. J Neurosci. 2007; 27:7541–7552. [PubMed: 17626215]

Whitman MC, Greer CA. Adult neurogenesis and the olfactory system. Prog Neurobiol. 2009; 89(2): 162–75. [PubMed: 19615423]

Zhang B, Wong M. Pentylenetetrazole-induced seizures cause acute, but not chronic, mTOR pathway activation in rat. Epilepsia. 2012; 53(3):506–11. [PubMed: 22242835]

Zeng LH, Xu L, Gutmann DH, Wong M. Rapamycin prevents epilepsy in a mouse model of tuberous sclerosis complex. Ann Neurol. 2008; 63(4):444–53. [PubMed: 18389497]

Zeng LH, Rensing NR, Wong M. The mammalian target of rapamycin signaling pathway mediates epileptogenesis in a model of temporal lobe epilepsy. J Neurosci. 2009; 29:6964–6972. [PubMed: 19474323]

Zeng LH, Bero AW, Zhang B, Holtzman DM, Wong M. Modulation of astrocyte glutamate transporters decreases seizures in a mouse model of Tuberous Sclerosis Complex. Neurobiol Dis. 2010; 37(3):764–71. [PubMed: 20045054]

Zhou J, Blundell J, Ogawa S, Kwon CH, Zhang W, Sinton C, Powell CM, Parada LF. Pharmacological inhibition of mTORC1 suppreses anatomical, cellular, and behavioral abnormalities in neuronal-specific *Pten* knockout mice. J Neurosci. 2009; 29:1773–1783. [PubMed: 19211884]

Highlights

- First direct evidence that selective disruption of the dentate gyrus causes epilepsy
- *PTEN* deletion from as few as 9% of granule cells is sufficient to cause epilepsy
- Findings suggest a plausible mechanism of epileptogenesis

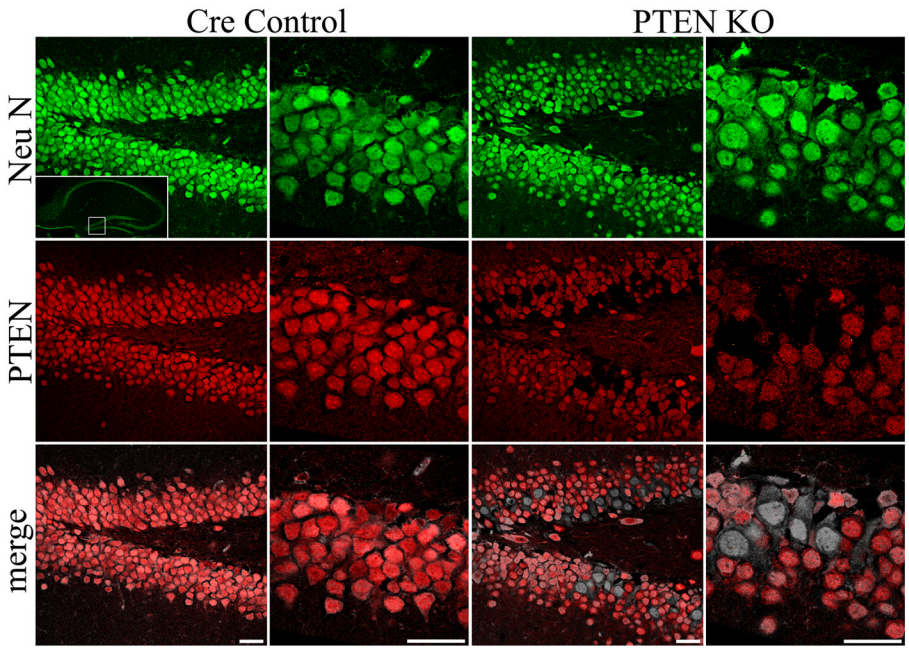

Figure 1.

Confocal optical sections of NeuN staining (green) reveal the dentate granule cell layer (boxed region in inset, top left panel) in cre control and PTEN KO mice treated with tamoxifen on P14. Sections were double-immunostained for PTEN (red), and in control animals, 100% of NeuN labeled granule cells also co-localize PTEN. In double transgenic mice, however, recombined granule cells appear as gaps in the PTEN staining. Note that these gaps correspond exactly with NeuN stained granule cells, and these PTEN-negative cells appear in black and white in the merged image. As expected, recombined granule cells were localized primarily to the inner region of the granule cell layer, where postnatally-generated granule cells are typically present. Scale bars = 25 μm. **S**ee also figures S1 and S2.

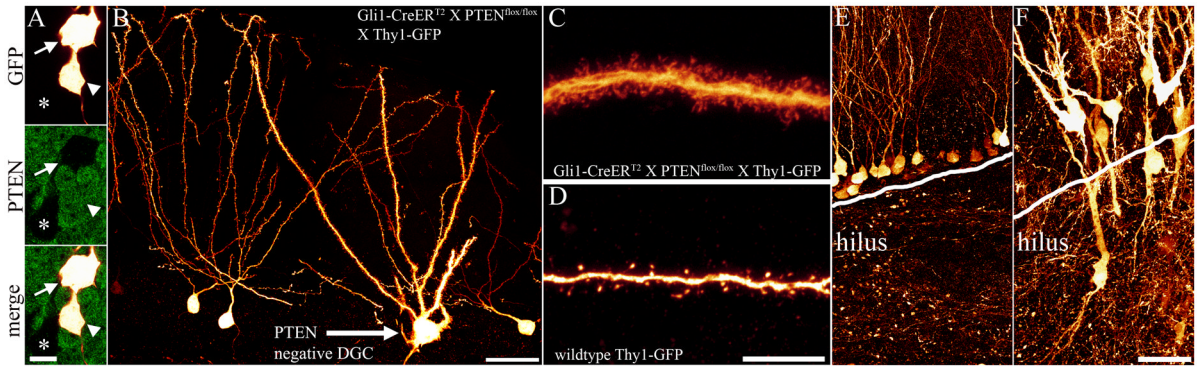

Figure 2.

A–D: Disrupted development of PTEN-immunonegative granule cells in Gli1-CreER^{T2} X PTEN$^{flox/flox}$ X Thy1-GFP mice. In these animals, the Thy1 promoter drives GFP expression in a subset of wildtype and PTEN KO granule cells. **A:** PTEN immunostaining of two GFP-expressing dentate granule cells. The upper cell (arrow) is PTEN-immunonegative, while the lower cell is immunoreactive for PTEN protein (arrowhead). The asterisk denotes a PTEN-negative, GFP-negative granule cell. **B:** Confocal maximum projection of a GFP-expressing, PTEN-negative granule cell (arrow) with GFP-expressing, PTEN-positive neighbors. Note how the PTEN-negative cell dwarfs its neighbors. **C,D:** Confocal maximum projections of GFP-labeled dendritic segments from PTEN-negative (C) and PTEN-positive (D) cells. The dendrite of the PTEN-negative cells exhibits dramatically increased thickness and spine density. **E,F:** GFP-expressing granule cells from cre control (E) and PTEN KO (F) mice. The white line in both images marks the dentate granule cell layer – hilar border. Note the presence of hilar ectopic granule cells in the KO. Scale bars = 10 μm (A), 30 μm (B), 25 μm (C), 20 μm (E,F).

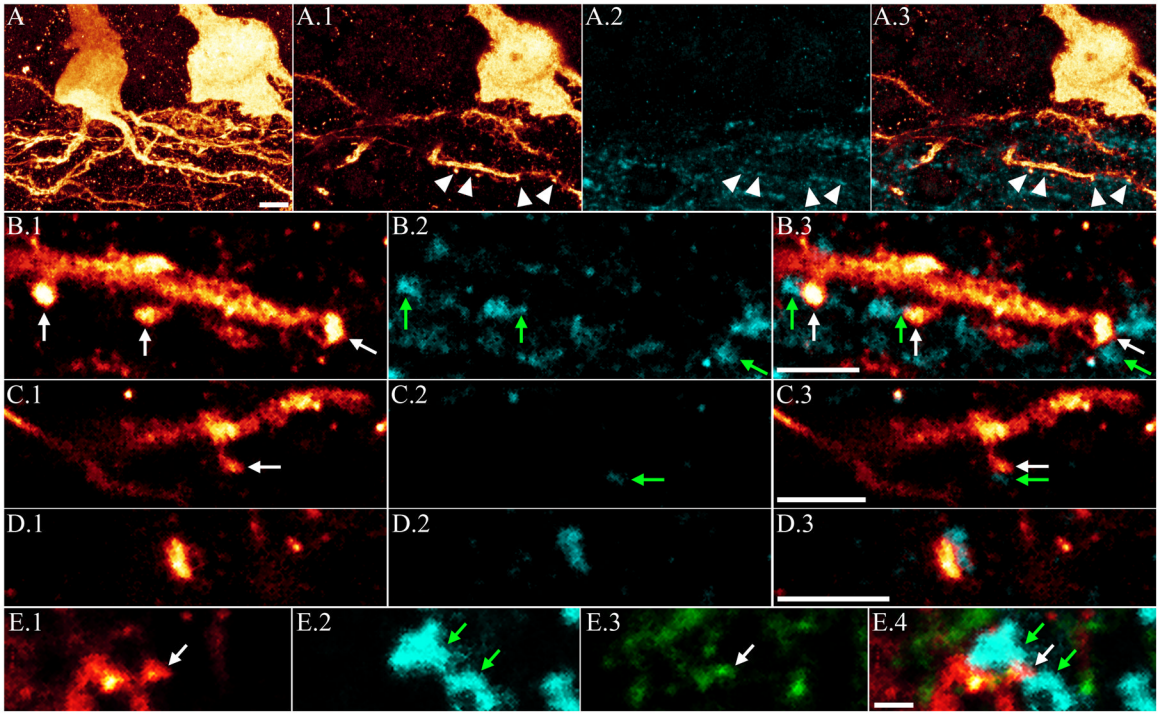

Figure 3.

A: Confocal maximum projection showing aberrant hilar basal dendrites on a PTEN KO granule cell. Single optical sections of these basal dendrites reveal dendritic spines (A.1) apposed to ZnT-3 immunoreactive puncta (arrowheads, A.2 and merged image in A.3) indicative of recurrent mossy fiber input. Higher resolution confocal optical sections of a subset of the spines shown in A are shown in B.1, with apposed ZnT-3 immunoreactive puncta in B.2, and merged images in B.3. White arrows denote spines and green arrows denote apposed puncta. Additional examples of basal dendrite spines and apposed ZnT-3 immunoreactive puncta are shown in C.1-C.3, and D.1-D.3. **E:** Confocal optical section of a basal dendrite spine in the hilus (E.1, white arrow) apposed to ZnT-3 immunoreactive puncta (E.2, green arrows). The spine is immunoreactive for PSD-95 (E.3, white arrow), providing further evidence of a functional synapse. Merged images are shown in E.4. Scale bars = 5 μm (A), 3 μm (B, C, D), 5 μm (E).

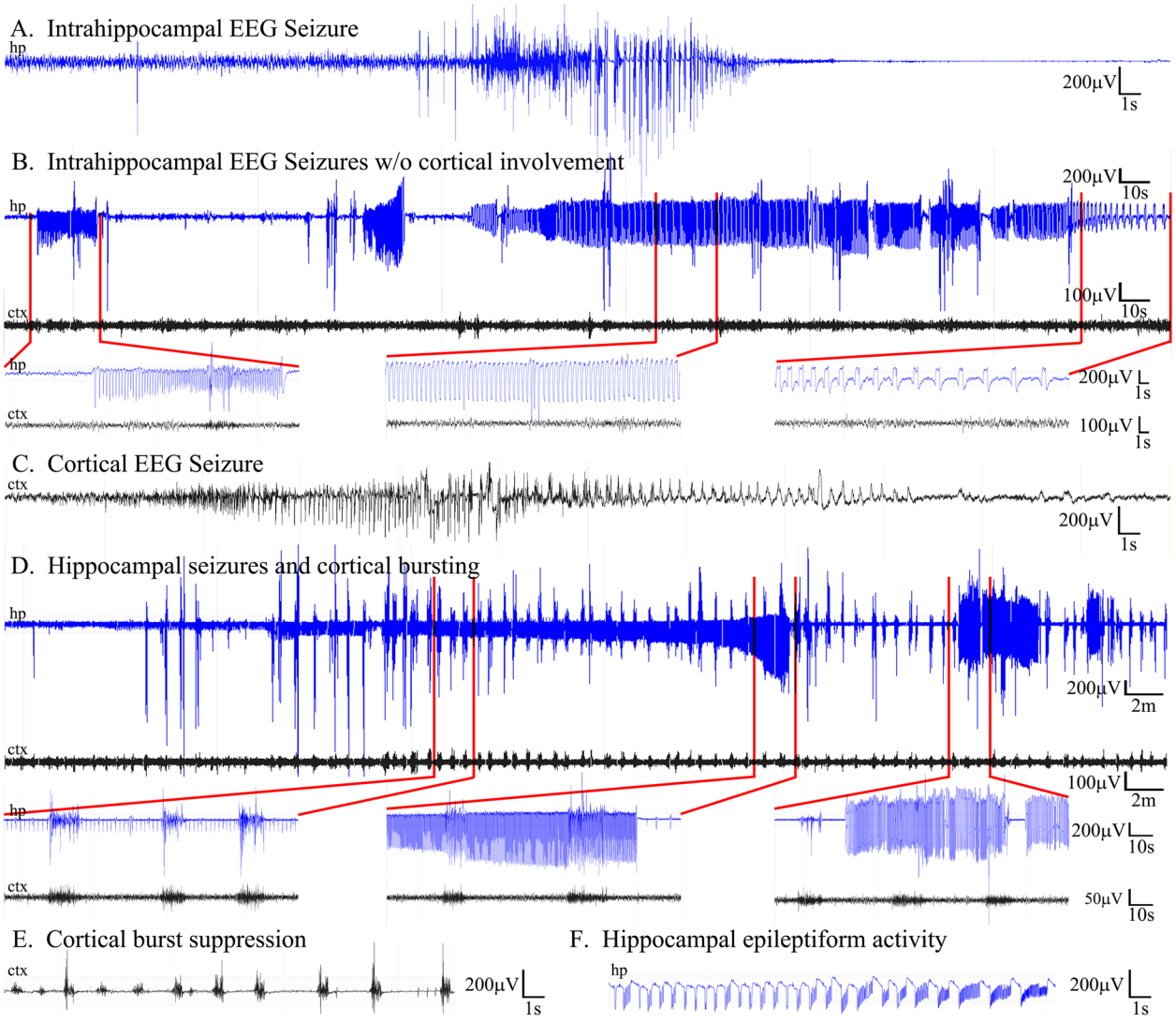

Figure 4.

PTEN KO mice treated with tamoxifen on P14 develop epileptic seizures. For all panels, cortical traces (ctx) are shown in black and hippocampal traces (hp) in blue. **A:** Typical electrographic seizure recorded using hippocampal depth electrodes. **B:** Dual trace EEG recording showing a long (≈3.5 minute) hippocampal seizure (hp, blue) preceded by two shorter seizures. Regions denoted by red lines are shown at higher resolution below. Note the absence of cortical involvement despite extensive hippocampal seizure activity. **C:** Example of a typical seizure recorded in cortex. **D:** Dual trace EEG showing seizure activity in cortex which gradually increases in amplitude over the course of the ≈30 minute event. In this trace, high amplitude intermittent burst activity is seen in both the hippocampal and cortical traces. **E:** Example of cortical burst suppression activity, which could persist for 30 minutes or longer and was typically observed as animal health declined. **F:** Example of epileptiform activity in hippocampus. See also figures S3 and S4.

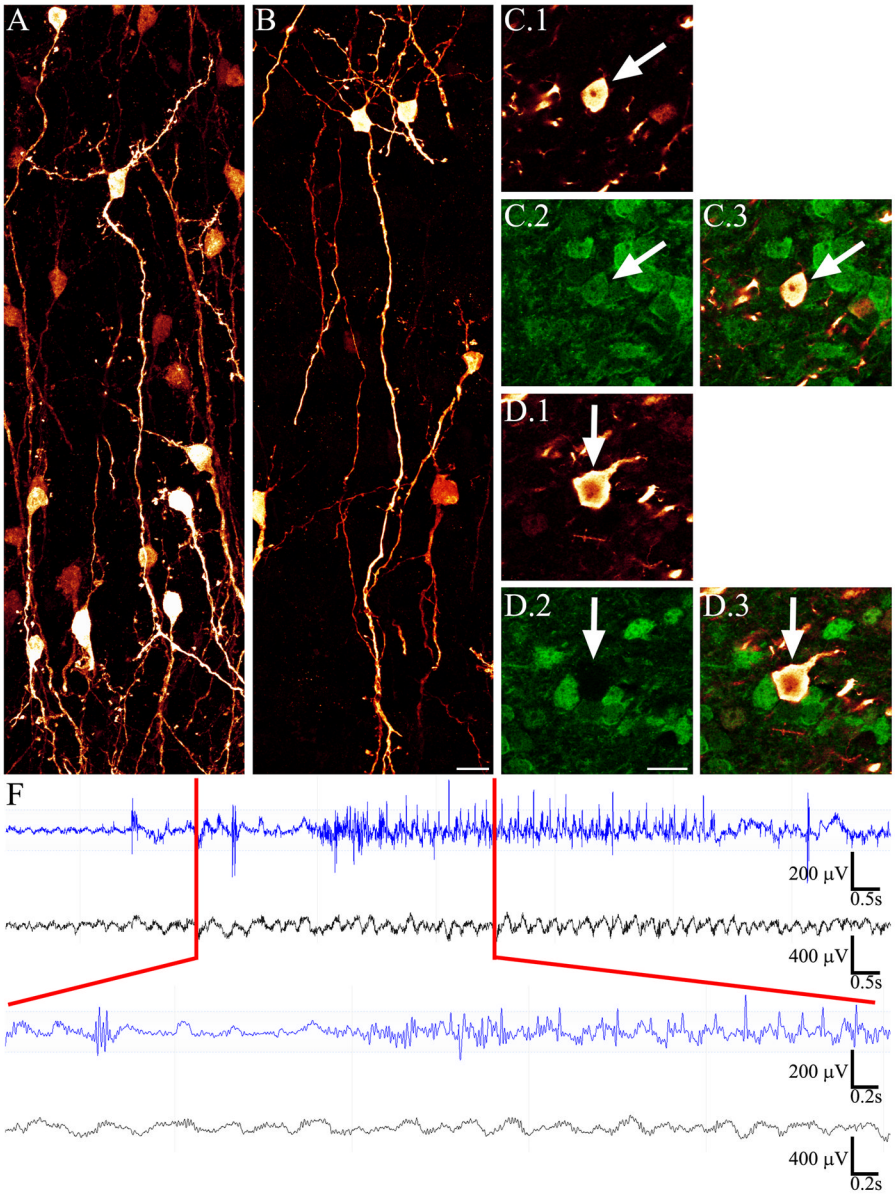

Figure 5.

Confocal maximum projections showing GFP-expressing olfactory granule neurons from control (A) and PTEN KO (B, C, D) mice. Olfactory granule cells from a PTEN KO animal immunostained for GFP and PTEN are shown in C and D. The cell in C (arrow) was immunoreactive for GFP (C.1) and PTEN (C.2), indicative of incomplete cre-mediated recombination in the cell (the GFP reporter was activated but at least one allele of PTEN was left intact). The cell in D (arrow) expressed GFP but was immunonegative for PTEN protein, indicative of complete recombination at all three lox-p splice sites. PTEN KO olfactory cells exhibited subtle, but statistically significant increases in soma area. Scale bars = 10 μm. **E:** Simultaneous EEG recording from hippocampus and olfactory bulb revealed epileptiform activity and seizures in the hippocampal trace (blue). Olfactory EEG (black) was unchanged during these events, and no seizures originating from, or isolated to, olfactory bulb were observed.

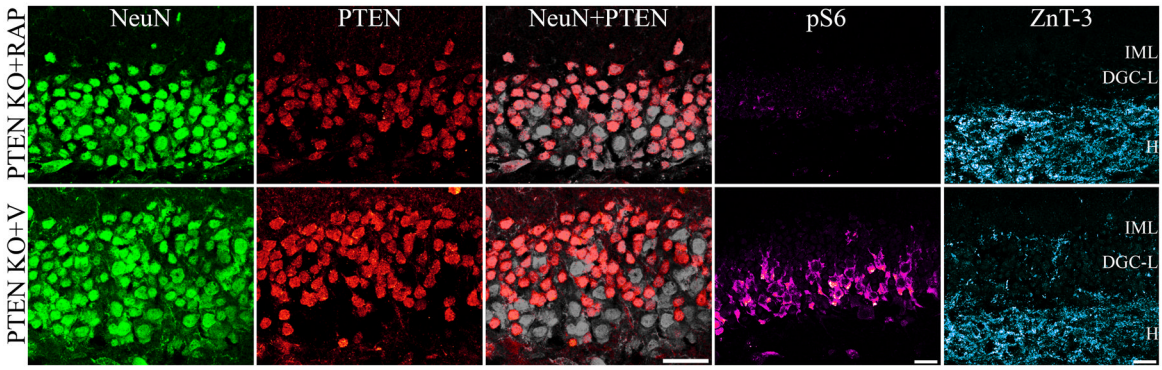

Figure 6.

Confocal maximum projections of NeuN (green) and PTEN (red) double-immunostaining reveal PTEN KO granule cells in animals treated with vehicle (V) or rapamycin (RAP). PTEN KO cells are shown in gray in the merged image. Confocal maximum projections showing pS6 staining (magenta) reveal robust staining in vehicle-treated PTEN KOs, and virtually absent staining in rapamycin treated animals. Confocal maximum projections showing ZnT-3 staining (cyan) demonstrate that rapamycin treatment was able to block the sprouting of mossy fiber axons into the dentate granule cell layer (DGC-L) and inner molecular layer (IML). Both groups exhibited the normal pattern of ZnT-3 staining in the dentate hilus (H). Scale bars = 25 μm.

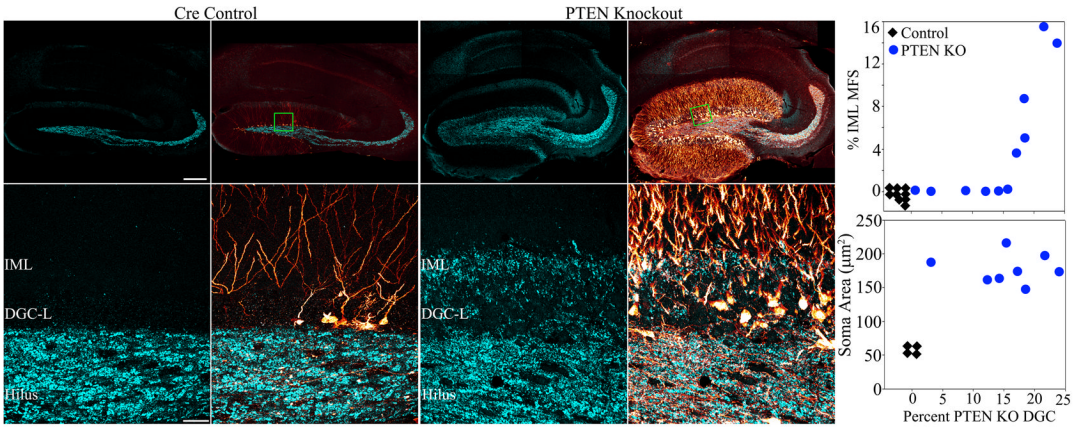

Figure 7.

Confocal maximum projections of hippocampi from tamoxifen-treated control and PTEN KO mice immunostained for GFP (red) and ZnT3 (cyan) are shown. ZnT3-labeling reveals the normal mossy fiber axon terminal field (hilus and stratum lucidum) in the control animal, while mossy fiber sprouting into the dentate granule cell layer (DGC-L) and inner molecular layer (IML) is evident in the knockout animal (green boxes in the top row correspond to high resolution images shown in the bottom row). Scale bars = 200 μm (top row) and 30 μm (bottom row). **Top graph:** Correlation between the degree of mossy fiber sprouting (assessed by ZnT3 immunoreactivity) in the IML and the percentage of PTEN KO granule cells. Control animals exhibited neither recombined cells nor mossy fiber sprouting (n=9, black diamonds), while mossy fiber sprouting in PTEN KO animals (blue circles) was significantly correlated with the percentage of recombined granule cells in the dentate gyrus ($P<0.01$). **Bottom graph:** PTEN KO granule cells exhibited somatic hypertrophy in all KO animals (n=8, blue dots) relative to GFP-expressing cells from cre-control animals (n=4, black diamonds), regardless of the degree of recombination or whether seizures were observed.

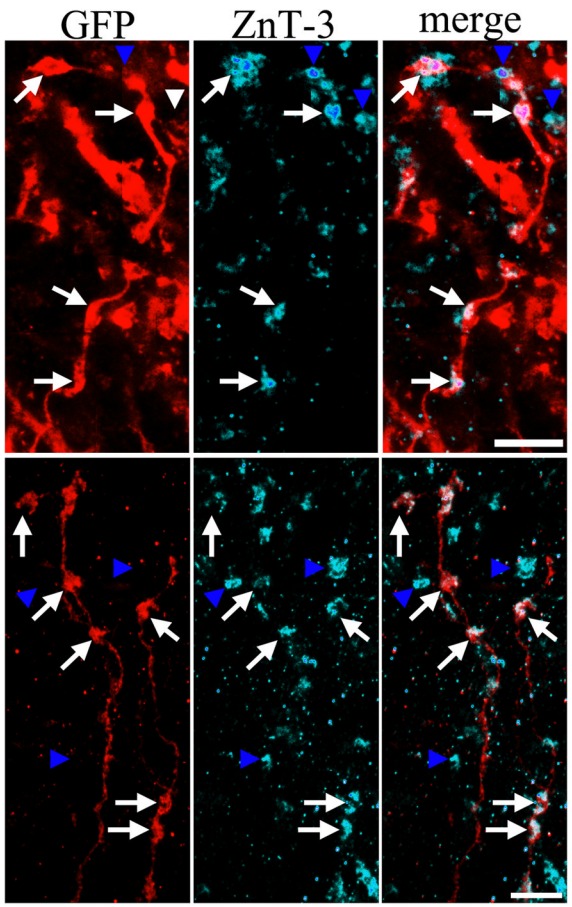

Figure 8.
Confocal optical sections of GFP-expressing mossy fiber axons in the dentate inner molecular layer from PTEN KO cells are shown in red. Double-immunostaining for the presynaptic granule cell terminal marker ZnT-3 is shown in cyan. White arrows denote ZnT-3 immunoreactive, GFP-expressing axon varicosities (presumptive PTEN KO cell axon terminals), while blue arrowheads denote ZnT-3 immunoreactive, GFP negative puncta (presumptive wildtype granule cell terminals). Scale bars= 5 μm.